scientific reports

Check for updates

OPEN

# Facile synthesis of acridine-based nickel(II) complexes *via* metal-mediated rearrangement of diphenylamine derivative and application in $H_2$ evolution reaction

Nutchanikan Phiromphu[1], Methasit Juthathan[1], Kittipong Chainok[2], Chatphorn Theppitak[2], Patchanita Thamyongkit[1], Thawatchai Tuntulani[1] & Pannee Leeladee[1]✉

**In this study, the formation of acridine-based metal complexes from rearrangement of diphenylamine-2,2′-dicarboxaldehyde (2,2′-dpadc) in the presence of transition metal ions was investigated. As a result, two novel isomorphic nickel(II) complexes bearing acridine-based Schiff-base ligand $[NiL^{ACR}](X)_2{\cdot}CH_3CN$ (X = $BF_4$ (1), $ClO_4$ (2), $L^{ACR}$ = (E)-$N^1$-(2-((acridin-4-ylmethylene)amino)ethyl)-$N^1$-(2-aminoethyl)ethane-1,2-diamine) were successfully synthesized *via* a one-pot condensation of 2,2′-dpadc and tris(2-aminoethyl)amine (TREN) with a satisfactory yield of approximately 60%. These complexes were fully characterized by X-ray crystallography, UV-vis spectroscopy and CHN elemental analysis. Additionally, their thermal stability (thermogravimetric analysis) and electrochemical properties were also determined. A plausible mechanism for the nickel(II)-mediated rearrangement of 2,2′-dpadc to form the acridine-based nickel(II) complex was proposed. To demonstrate their potential applications, complex 1 was explored in the realm of electrocatalysis. It exhibited moderate activity towards hydrogen evolution reaction (HER). During 1-h controlled-potential electrolysis (CPE) experiments, $H_2$ production (16 micromole) was observed with faradaic efficiency of 40% when the reaction was conducted in a $TBAPF_6$/DMF solution at -2.1 V vs. $Fc/Fc^+$ in the presence of acetic acid as a proton source. The facile synthesis of these acridine-based nickel(II) complexes reported herein may stimulate further development of novel acridine-based ligands and their corresponding metal complexes for a wide range of applications.**

Acridine-based compounds have garnered significant attention due to their diverse applications. For instance, a range of substituted 9-aminoacridine derivatives have demonstrated potent chemotherapeutic activity against pancreatic cancer[1,2]. Acridine-based compounds were also employed as chemical sensors thanks to their fluorescent properties[3–6]. While acridine derivatives have been extensively studied in sensing and biological applications, acridine-based metal complexes as catalysts remain relatively less explored. Among these, pincer-type ruthenium complexes have emerged as prominent catalysts in organic transformations. A notable example is the acridine-based PNP-pincer Ru complex, RuHCl(CO)(A-$^i$Pr-PNP) [A-$^i$Pr-PNP = 4,5-bis-(diiso-propylphosphinomethyl)acridine], which has been shown to catalyze the selective coupling of alcohols with ammonia to yield primary amines, as well as the catalytic conversion of primary alcohols to acetals and esters[7–9]. Furthermore, the acridine-based ruthenium(II) complex was employed in the direct preparation of *N*-heteroaromatics (i.e., *N*-substituted pyrroles and pyrazine derivatives) through dehydrogenative coupling of diols[10].

Given the importance of acridine compounds in various applications, considerable efforts have been dedicated to developing efficient synthetic methodologies. The Bernthsen reaction, involving the condensation of diphenylamine with a carboxylic acid and zinc chloride ($ZnCl_2$) at elevated temperatures (> 200 °C) over extended periods (up to 24 h), is a straightforward synthesis of acridine compounds[11–14]. It has been proposed that the presence of Lewis acid catalysts (e.g., $AlCl_3$, $ZnCl_2$, $FeCl_3$) facilitates the rearrangement of diphenylamine

[1]Department of Chemistry, Faculty of Science, Chulalongkorn University, Bangkok 10330, Thailand. [2]Thammasat University Research Unit in Multifunctional Crystalline Materials and Applications (TU-McMa), Faculty of Science and Technology, Thammasat University, Pathum Thani 12121, Thailand. ✉email: pannee.l@chula.ac.th

with an aldehyde or imine functional group at the 2-position of the phenyl ring. The compound with either the aldehyde or imine moiety, coordinated to the Lewis acid, undergoes cyclization followed by aromatization to yield the acridine core. While this method is well-established, it often suffers from harsh reaction conditions. Interestingly, a seminal work by Brooker and co-workers demonstrated the synthesis of the first example of tetrahedral acridine-based Schiff base cobalt(II) complexes (Fig. 1c) through a cobalt(II)-mediated rearrangement of diphenylamine-2,2′-dicarboxaldehyde (2,2′-dpadc, Fig. 1a) under mild conditions[15]. This discovery has opened up new avenues for the exploration of metal-mediated synthetic strategies for acridine derivatives. In our view, this facile method would allow us to further explore this class of ligands, especially in catalytic applications, by incorporation of various transition metals. In addition, this could also be a greener route for synthesis of acridine-based compounds due to its mild condition.

In this study, we investigated the formation of acridine-based metal complexes through the rearrangement of 2,2′-dpadc in the presence of various transition metal ions. This approach led to the successful synthesis and characterization of two novel pentadentate nickel(II) compounds featuring acridine-based Schiff-base ligands, $[NiL^{ACR}](X)_2 \cdot CH_3CN$ (X = $BF_4$ (**1**), $ClO_4$ (**2**), $L^{ACR}$ = (E)-$N^1$-(2-((acridin-4-ylmethylene)amino)ethyl)-$N^1$-(2-aminoethyl)ethane-1,2-diamine, Fig. 1d). To the best of our knowledge, this nickel(II) complex represents the second example of a metal-mediated rearrangement from 2,2′-dpadc to form an acridine-based metal complex. Our work further supports the viability of metal-mediated approaches as promising alternatives for the synthesis of acridine-based compounds. Additionally, the potential application of the nickel(II) complex in electrocatalytic hydrogen evolution reaction (HER) was also demonstrated.

## Experimental section

### Materials and methods

All reagents were used as received without further purification unless otherwise stated. Solvents used for syntheses were reagent grade except acetonitrile, which was HPLC grade. 2,2′-iminodibenzoic acid (95%), manganese(IV) oxide (activated, 85%), nickel(II) perchlorate hexahydrate (99%), tris(2-aminoethyl)amine (TREN, 96%), tetrabutylammonium hexafluorophosphate (98%), and Celite® filter cel (filter aid, slightly calcined) were obtained from Sigma Aldrich. Lithium aluminum hydride (95%) was purchased from TCI. Nickel(II) tetrafluoroborate hexahydrate (99%) was obtained from ACROS. Glassy carbon electrode and non-aqueous Ag/$AgNO_3$ reference electrode were purchased from CH Instrument Inc.

Nuclear magnetic resonance (NMR) spectra were recorded on a 500 MHz JEOL at 298 K. UV-vis spectra were recorded on a Varian Cary 50 probe UV-vis spectrophotometer. Elemental analyses (C, H, N) were determined

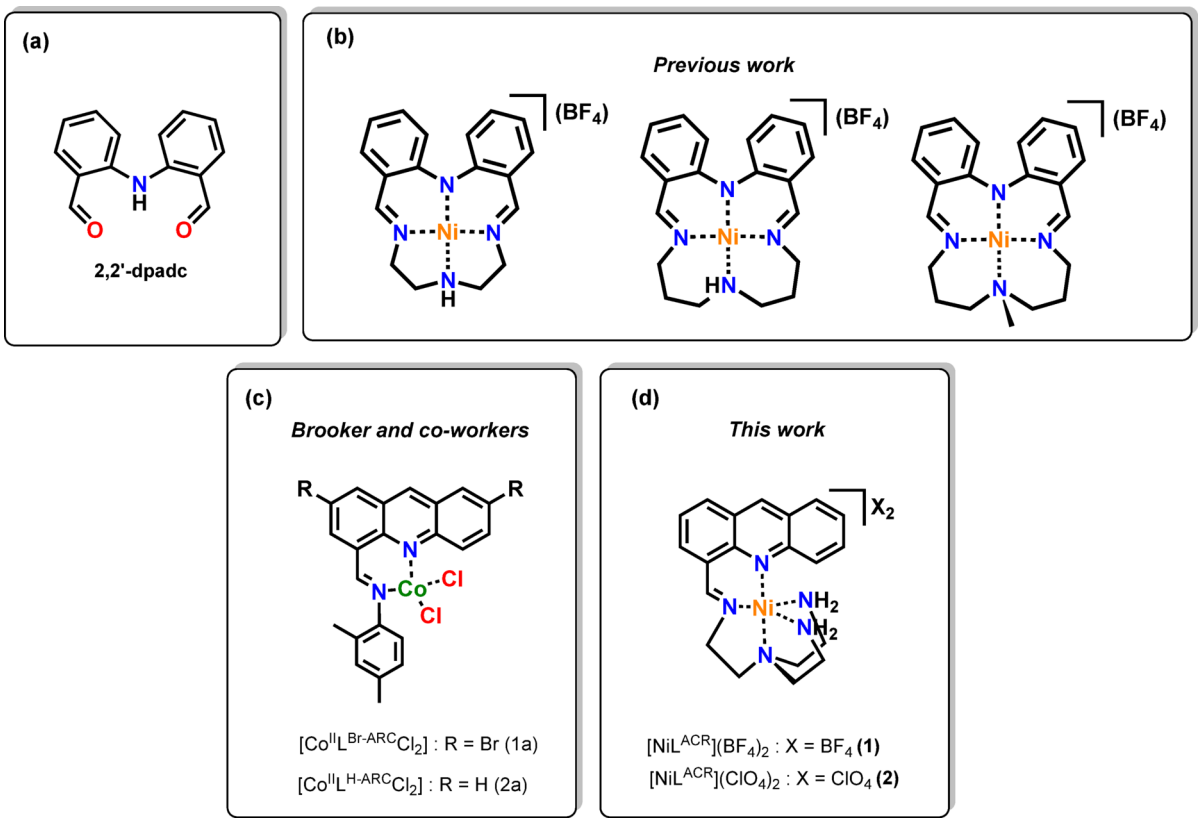


**Fig. 1**. Chemical Structure of (**a**) 2,2′-dpadc, (**b**) nickel(II) complexes featuring $N_4$-Schiff base macrocycle ligands[16], (**c**) acridine-based cobalt(II) complexes from diphenylamine-based precursors[15], (**d**) nickel(II) complexes bearing Schiff-base acridine-based ligand in this work.

by THERMO FLASH 2000 CHNS/O analyzers. Thermogravimetric analyses (TGA) were carried out with a TGA 55 TA Instrument in the temperature range of 30–800 °C under a nitrogen atmosphere flow with a heating rate of 10 °C $min^{-1}$. Cyclic voltametric measurements were conducted using Metrohm-Autolab (Model PGSTAT101).

## Acridine-based Schiff-base metal complexes from metal-mediated rearrangement of 2,2′-dpadc

In a typical reaction, to a bright-yellow, refluxing solution of 2,2′-dpadc (135 mg, 0.60 mmol) in $CH_3CN$ (10 mL) was added metal salts (0.60 mmol) dissolved in $CH_3CN$ (10 mL) (metal salts = $Ni(BF_4)_2{\cdot}6H_2O$, $Ni(ClO_4)_2{\cdot}6H_2O$, $Fe(acac)_3$, $Co(BF_4)_2{\cdot}6H_2O$, $Cu(BF_4)_2{\cdot}6H_2O$, or $Cu(ClO_4)_2{\cdot}6H_2O$ (*Caution: perchlorate is potentially explosive, so the experiment should be carefully handled.*). Then, a solution of TREN (88 mg, 0.60 mmol) in $CH_3CN$ (10 mL) was added dropwise over 20 min. Thanks to a characteristic absorption band of the acridine moiety around 360 nm[17], formation of the acridine-based ligand during the reaction was monitored by UV-vis spectroscopy. After refluxing for a certain period of time (3–24 h), the solvent was removed under reduced pressure. If applicable, the product was then crystallized by liquid-liquid diffusion ($CH_3CN$/diethyl ether).

**$[NiL^{ACR}](BF_4)_2$ (1)** was obtained as dark brown block-shaped crystals (56%). Anal. Calc. for $[C_{20}H_{25}B_2F_8N_5Ni]$: C 42.31, H 4.44, N 12.34%. Found: C 42.32, H 4.59, N 12.56%. $\lambda_{max}$/nm ($\varepsilon_{max}$/ $M^{-1}$ $cm^{-1}$) = 291 (8800), 344 (6800), 360 (11000), 387 (6800), 403 (7250). ESI-MS (m/z) of $[C_{20}H_{25}N_5Ni]^{2+}$ for calculated: 196.57290; found: 196.57335.

**$[NiL^{ACR}](ClO_4)_2$ (2)** was obtained as dark brown block-shaped crystals (61%). Anal. Calc. for $[C_{20}H_{25}Cl_2N_5NiO_8]$: C 40.51, H 4.25, N 11.81%. Found: C 40.55, H 4.33, N 12.12%. $\lambda_{max}$/nm ($\varepsilon_{max}$/ $M^{-1}$ $cm^{-1}$) = 291 (9100), 344 (7000), 360 (11500), 387 (7100), 403 (7500).

*X-ray crystallography*

Suitable crystals of complexes **1** and **2** were mounted on MiTeGen micromounts using paratone oil. X-ray diffraction data were collected using a Bruker D8 Quest Cmos Photon II operating at T = 296(2) K. Data were collected using ω and ϕ scans and using Mo-Kα radiation (λ = 0.71073 Å). The total number of runs and images was based on the strategy calculation from the program APEX3 and unit cell indexing was refined using SAINT[18]. Data reduction was performed using SAINT and SADABS were used for absorption correction. The integrity of the symmetry was checked by using PLATON[19]. The structure was solved with the ShelXT structure solution program using combined Patterson and dual-space recycling methods[20]. The structure was refined with a full-matrix least squares on $F^2$ using ShelXL[21] and OLEX2[22]. In the final refinement cycles, all non-hydrogen atoms were refined anisotropically. The hydrogen atoms were introduced in calculated positions and refined with fixed geometry and riding thermal parameters with respect to the carrier atoms. A summary of the crystal data and relevant refinement parameters is presented in Table 1. CCDC 2,130,819 (**1**) and 2,130,820 (**2**), contain the supplementary crystallographic data for this study. These data can be obtained free of charge from The Cambridge Crystallographic Data Centre via www.ccdc.cam.ac.uk/data_request/cif.

| Compound | 1 | 2 |
|---|---|---|
| Empirical Formula | $C_{22}H_{28}N_6B_2F_8Ni$ | $C_{22}H_{25}Cl_2N_6NiO_8$ |
| Formula Weight | 608.83 | 634.11 |
| Temperature (K) | 296(2) | 296(2) |
| Wavelength (Å) | 0.71073 | 0.71073 |
| Crystal System | triclinic | triclinic |
| Space Group | *P*-1 | *P*-1 |
| *a* (Å) | 8.2720(3) | 8.3309(3) |
| *b* (Å) | 10.0320(3) | 10.1513(3) |
| *c* (Å) | 16.1128(5) | 16.2660(5) |
| *α* (°) | 86.663(1) | 86.568(1) |
| *β* (°) | 87.204(1) | 86.593(1) |
| *γ* (°) | 84.311(1) | 83.398(1) |
| V ($Å^3$) | 1327.03(7) | 1362.12(8) |
| Z | 2 | 2 |
| $\rho_{calc}$ ($g/cm^3$) | 1.524 | 1.546 |
| $\mu$ ($mm^{-1}$) | 0.81 | 0.965 |
| Reflns collected/unique | 46,995/6601 | 37,998/6762 |
| GOF on $F^2$ | 1.017 | 1.049 |
| $R_{int}$, $R_{sigma}$ | 0.078, 0.0457 | 0.0269, 0.0175 |
| $R_1$, $wR_2$ [$I > 2\sigma(I)$] | 0.0451, 0.0909 | 0.0501, 0.1446 |
| $R_1$, $wR_2$ (all data) | 0.0770, 0.1047 | 0.0561, 0.1512 |
| Max./min. residual (e $Å^{-3}$) | 0.49/−0.29 | 0.89/−0.68 |
| CCDC No. | 2,130,820 | 2,130,819 |

**Table 1**. Crystal data and structural refinement for **1** and **2**.

### Homogeneous electrochemical studies of $[NiL^{ACR}](BF_4)_2$ (1)

The redox property of complex **1** (1 mM) in dimethylformamide (DMF) was examined by cyclic voltammetry (CV) using tetrabutylammonium hexafluorophosphate ($TBAPF_6$) (0.1 M) as a supporting electrolyte. The measurements were performed using a conventional three-electrode one-component configuration in which the working electrode and the reference electrode was a glassy carbon electrode (diameter = 0.3 cm, A = 0.71 $cm^2$) and an $Ag/AgNO_3$ (10 mM) electrode, respectively, and a platinum wire was used as a counter electrode. The measured potentials were quoted with respect to the $AgNO_3$/Ag electrode and internally calibrated to $Fc/Fc^+$ redox couple. The experiments were carried out at 25 °C under $N_2$ atmosphere. The current (i) at a glassy carbon working electrode was recorded at various scan rates of 0.05–1.00 V/s after applying voltage (E).

To investigate HER activity of **1**, the electrocatalytic performance of complex **1** was measured in $N_2$-saturated DMF/0.1 M $TBAPF_6$ with various concentrations of acetic acid (0–30 mM) as a proton source. The measurements were carried out in a three-electrode system in a H-type cell with the anodic chamber (containing working and counter electrodes) and cathodic chamber (containing reference electrode) as illustrated in Figure S7.

The generated current corresponding to the catalytic HER activity of complex **1** was also recorded and plotted against the applied potential. Furthermore, controlled-potential electrolysis (CPE) was performed in the same electrochemical apparatus with the continuous stirring in both chambers during electrolysis. At the end of the electrolysis, aliquots of headspace gas (4 mL) from the cathodic chamber were collected and analyzed by gas chromatograph (Agilent Technologies 8890 GC instrument coupled with TCD detector, He carrier gas).

## Results and discussion

### Formation of pentadentate nickel(II) complexes bearing acridine-based Schiff-base ligand through rearrangement of 2,2′-dpadc

It has been previously reported that the metal complexes with diphenylamine-based Schiff-base metal macrocycles could be synthesized through a one-pot reaction of metal-templated [1 + 1] Schiff-base condensation[23,24]. Therefore, along with our study of nickel(II) complexes featuring $N_4$ Schiff-base macrocycles (Fig. 1b)[16], we initially intended to synthesize penta-coordinated Schiff-base nickel(II) macrocycles $(NiL^{N5MCC})^+$ through this synthetic route using the same head unit (*i.e.*, 2,2′-dpadc) to react with TREN in the presence of nickel(II) salts (i.e., $Ni(BF_4)_2$, or $Ni(ClO_4)_2$) (Fig. 2). To our surprise, the crystallographic data, however, revealed an unexpected formation of acridine-based nickel(II) Schiff-base complexes, $[NiL^{ACR}](BF_4)_2$ (**1**) and $[NiL^{ACR}](ClO_4)_2$ (**2**) (Fig. 1d).

*Structural descriptions*

X-ray quality crystals were obtained by slow diffusion of diethyl ether into the solution of complexes in acetonitrile. The single crystal X-ray diffraction analyses reveal that complexes **1** and **2** are isostructural and crystallize in the centrosymmetric triclinic system with space group *P*-1 (Table 1). The asymmetric unit consists of one crystallographic unique nickel(II) ion, two counter anions, and one lattice acetonitrile molecule. The molecular structure of cationic species of the complex is shown in Fig. 3. The central nickel(II) ion is five-coordinated with a distorted trigonal bipyramidal geometry surrounded by five nitrogen atoms from the ligand, in which N1 and N3 atoms occupy the axial positions, while three basal positions being taken up by N2, N4, and N5 atoms. The Ni – N bond lengths are in the range of 1.957(2)-2.110(2) for **1** and 1.967(2)-2.115(2) Å for **2** (Table S1), which are comparable to those reported in other related nickel(II) complexes[25–27].

A close inspection of the crystal structure discloses that a pair of symmetry-related $[NiL^{ACR}]^{2+}$ complexes are stacked through face-to-face π – π interactions exist between acridine moieties of the $L^{ACR}$ ligands to from a supramolecular dimeric structure (centroid-to-centroid distances = 3.865(3) – 3.924(3) Å for **1**,

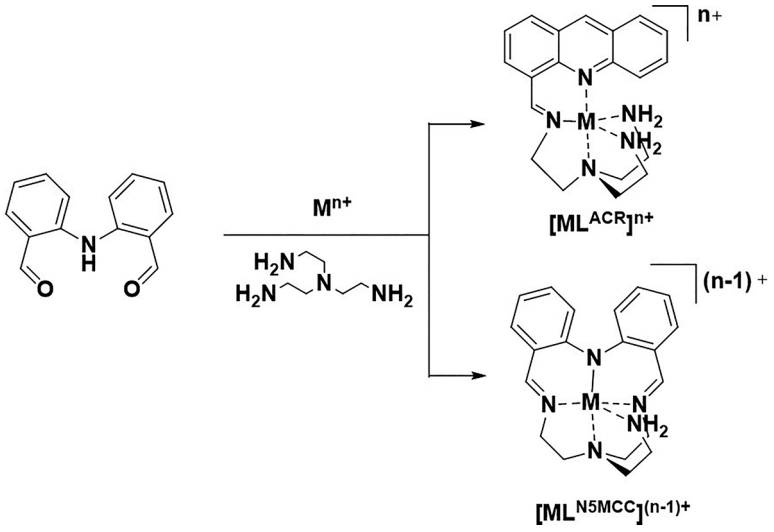


**Fig. 2**. Possible reaction between 2,2′-dpadc and TREN in the presence of metal ions.

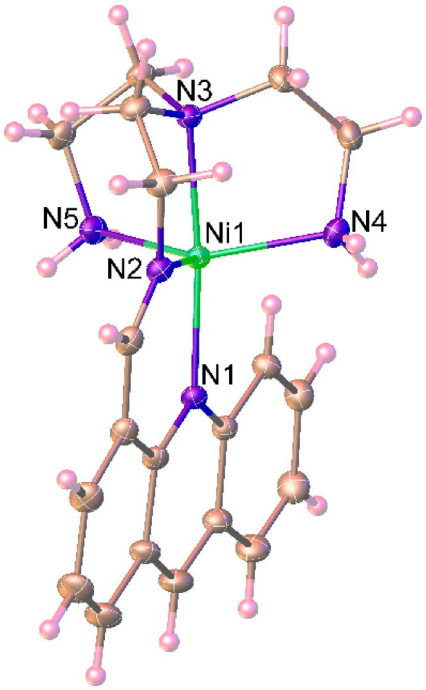


**Fig. 3**. ORTEP diagram of $[NiL^{ACR}]^{2+}$ showing the coordination environment for nickel(II) atom in **1**. The atoms are represented by 50% probability thermal ellipsoids.

3.866(2) – 3.921(2) Å for **2**). The dimers are assembled into a one-dimensional column structure by N – H···F/O hydrogen bonds between the amine groups of the ligands and the counter anions, Fig. 4. Ultimately, the columns are interconnected with counter anions and lattice acetonitrile molecules through complementary N – H···F/O and C – H···F/O hydrogen bonding interactions, giving rise to a three-dimensional supramolecular architecture. Details of the hydrogen bonding geometry for the complexes **1** and **2** are given in Table S2.

*Electronic and electrochemical properties of acridine-based nickel(II) complexes*

UV-vis spectra of the two nickel(II) complexes showed the identical absorptions (in agreement with their isostructure) at 291, 344, 360, 387, and 403 nm which could be assigned to charge transfer transitions (Fig. 5)[6,18]. It should be noted that the characteristic absorption band of the acridine moiety in the complexes was observed at ca. 360 nm, consistent with the previous report[6]. However, no *d-d* transition band was clearly seen, probably due to its lower absorptivity with respect to that of the ligand.

The cyclic voltametric measurements of nickel(II) complexes were conducted in a $N_2$-saturated DMF solution containing 0.1 M $TBAPF_6$ (Figure S5). The cyclic voltammogram of **1** exhibited two irreversible processes at E = -1.18 V and E = -0.45 V for reduction ($E_{pc,1}$) and oxidation events ($E_{pa,1}$), respectively. Moreover, at more negative potentials, a quasi-reversible process was observed at $E_{1/2}$ = -1.89 V. Likewise, the cyclic voltammogram of **2** showed the redox events in negative potentials at E = -0.48 V and – 1.19 V for irreversible process, and at $E_{1/2}$ = -1.90 V for a quasi-reversible process. These similar redox potentials and peak shapes indicate their similar electronic properties, which is consistent with the alike structural configuration.

*Proposed mechanism of acridine-based complex formation*

According to the previous reported cobalt(II) mediated rearrangement of diphenylamine-based starting materials[18], a similar mechanism of acridine formation for our nickel(II) complexes *via* rearrangement of 2,2′-dpadc was proposed as depicted in Fig. 6. Firstly, 2,2′-dpadc was reacted with tris(2-aminoethyl)amine (TREN) *via* Schiff base condensation, resulting in one imine arm. Next, the imine arm was activated by the nickel(II), providing more electrophilicity of the carbon atom in the imine which hereafter underwent a 6-membered cyclization. Thereafter, a couple of deprotonations took place to rearomatize and formed the acridine with a pendant carbonyl arm meanwhile releasing nickel(II) salt and TREN back into the solution. The carbonyl-dangling acridine and TREN were further subjected to nickel-templated Schiff-base condensation which ultimately formed the acridine-based Schiff-base Ni(II) complex.

## Investigation of rearrangement of 2,2′-dpadc mediated by various metal ions

To explore whether this nickel(II)-mediated rearrangement is applicable to other metal ions, a range of transition metal salts was tested. Unfortunately, when monitoring the reaction with $Co(BF_4)_2$, $Fe(acac)_3$ or $BF_3$ (non-metal Lewis acid), characteristic absorption of the acridine moiety at 360 nm was not observed (Figure S1). This indicated that these two metal salts as well as $BF_3$ may not be able to induce the rearrangement to form

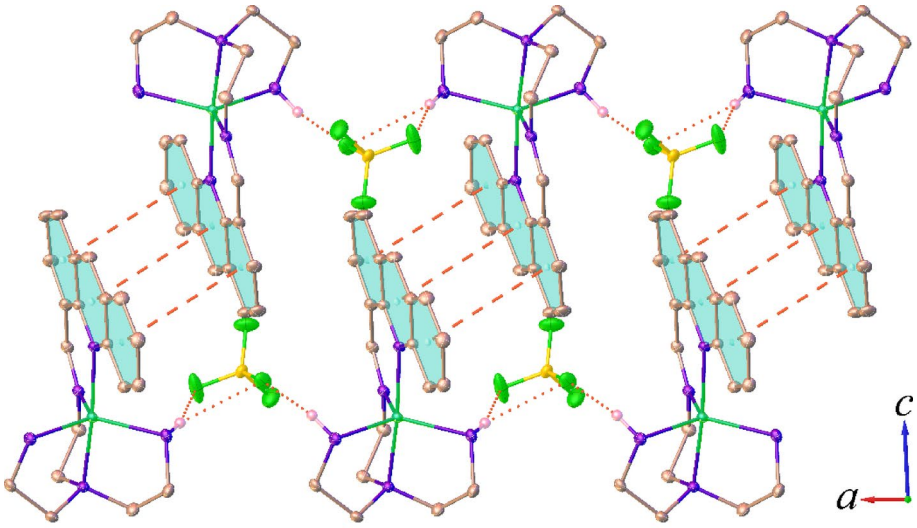


(a)

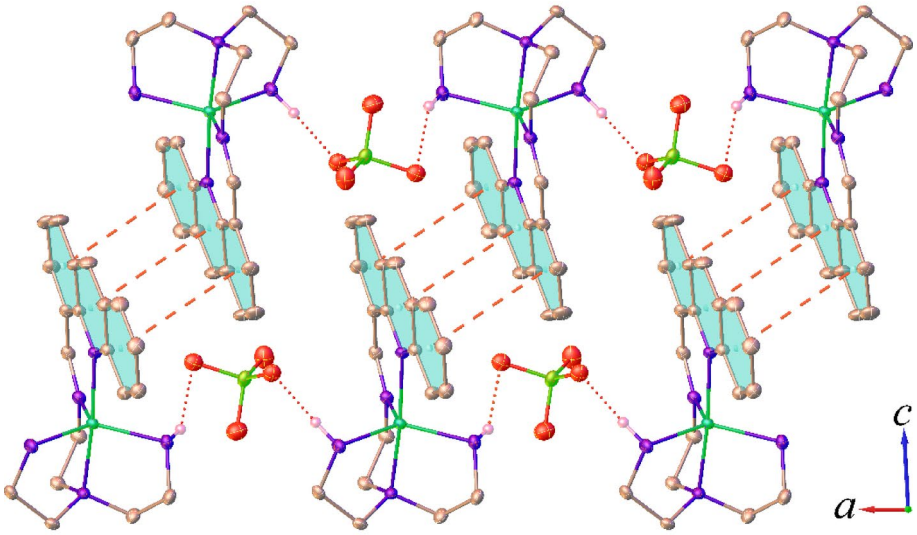


(b)

**Fig. 4**. Views of the one-dimensional column structures forming by the complementary hydrogen bonding and π-π stacking interactions in **1** (**a**) and **2** (**b**).

an acridine-based ligand. Also, attempts to identify the product from these reactions resulted in unidentified substances.

Interestingly, when $Cu(BF_4)_2$ was employed in the reaction, $[CuL^{N5MCC}](BF_4)$ ($L^{N5MCC}$ = $N_5$-donor macrocyclic ligand) was obtained, and no indication of acridine formation was observed. Although attempts to obtain single crystals suitable for X-ray crystallography have not been successful, the copper(II) complex could be confirmed by UV-vis spectroscopy and mass spectrometry (ESI-MS). Markedly, the UV-vis spectrum of $[CuL^{N5MCC}](BF_4)$ in $CH_3CN$ is similar to that of the previously reported $[CuL^{Et}](BF_4)$[28,29] with a small bathochromic shift of 10–20 nm. On the other hand, when $Cu(ClO_4)_2$ was used as the metal source, a mixed product of $[CuL^{ACR}(ClO_4)]^+$ and $[CuL^{N5MCC}]^+$ was evidenced by UV-vis spectroscopy and ESI-MS. Unfortunately, the pure product of $[CuL^{ACR}(ClO_4)]^+$ could not be obtained for further characterization.

It can be seen that among the metal salts used in this work, only $Ni(BF_4)_2$ and $Ni(ClO_4)_2$ can mediate the rearrangement of 2,2′-dpadc in the reaction with TREN to give the purified product of acridine-based metal complexes, *i.e.* complex **1** and **2**. The origin of exclusivity of the $Ni^{2+}$ ions in this particular reaction may be attributed to the size and Lewis acidity of $Ni^{2+}$ ions, but it has not been clearly understood. Further studies such

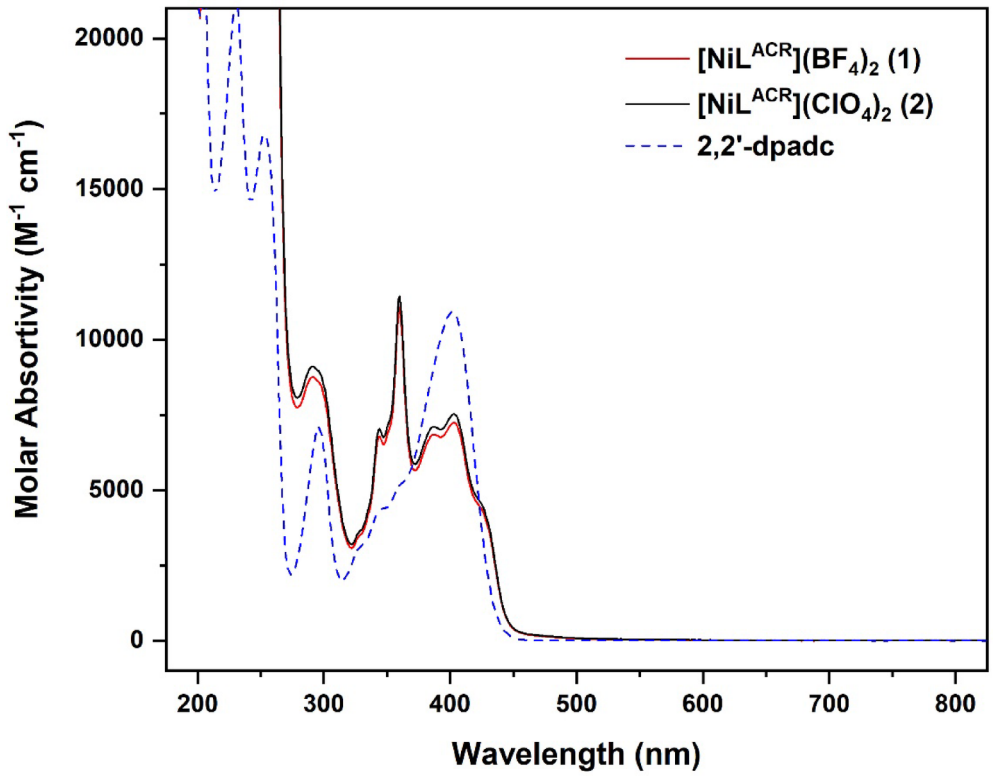


**Fig. 5**. UV-vis spectroscopic characterization of 0.1 mM $[NiL^{ACR}](BF_4)_2$ (**1**, red solid line) $[NiL^{ACR}](ClO_4)_2$ (**2**, black solid line), and 2,2′-dpadc in acetonitrile solution (blue dashed line).

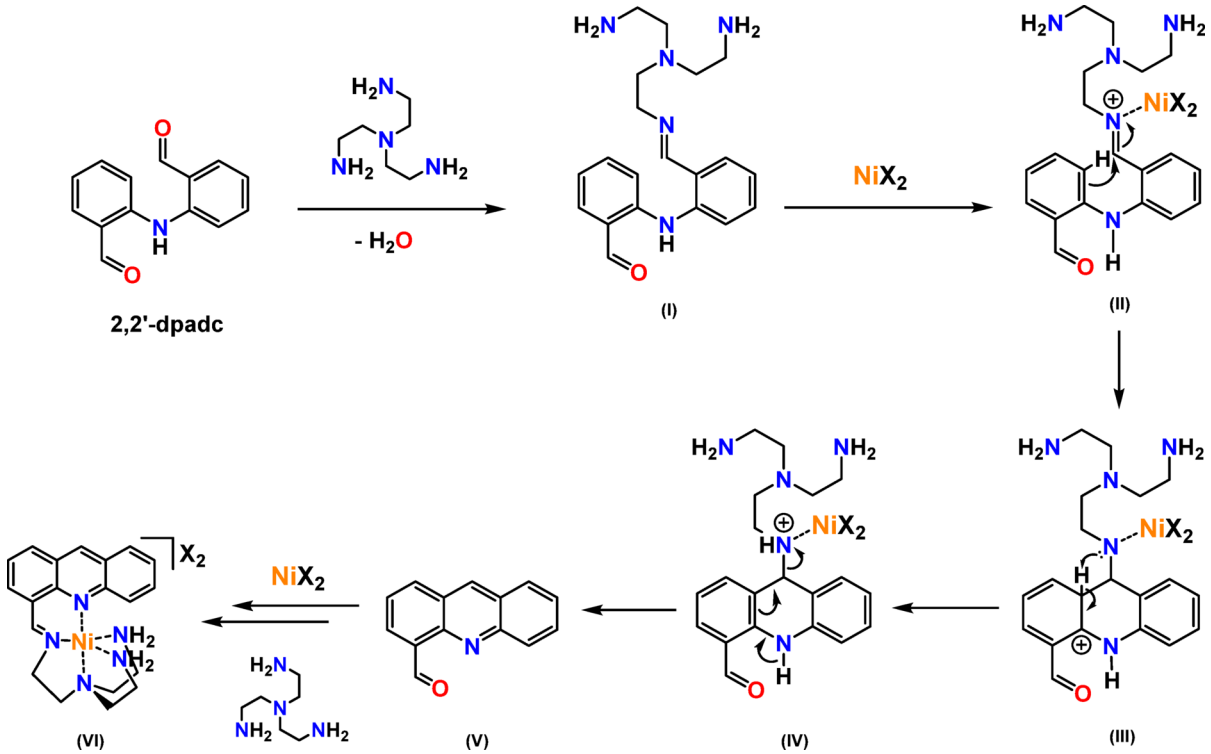


**Fig. 6**. Plausible mechanism of nickel-mediated acridine-based ligand formation.

as DFT calculations are needed to get deeper insight into this reaction. Thus, the studies regarding their potential application hereafter would focus on the nickel(II) complex. From the literature, a number of nickel(II) complexes with imine derivative ligands have been reported and used in various applications[30–34]. In particular, several Ni(II) complexes and materials have been demonstrated as potential electrocatalysts for hydrogen evolution reaction (HER)[35,36]. Due to the importance of HER in addressing energy and environmental challenges, it is of interest to further investigate the potential of the nickel(II) complex (**1**) in this particular application.

### Electrocatalytic hydrogen evolution reaction (HER) of complex 1

Due to their similarity in the structure and properties, further studies regarding the HER activity of acridine-based nickel(II) complexes were concentrated only on complex **1**. Firstly, complex **1** was examined whether it could be an active HER electrocatalyst in comparison to $Ni(BF_4)_2$. CVs of the complex **1** were performed in a $N_2$-saturated 0.1 M $TBAPF_6$ /DMF solution. Upon addition of acetic acid (0–30 mM) as the proton source, catalytic current enhancement around the reduction peak of $Ni^{2+}$/ $Ni^{+}$ in complex **1** was clearly observed and significantly higher than that of $Ni(BF_4)_2$. Next, the CPE was conducted at applied potential ($E_{applied}$) of -2.1 V vs. $Fc/Fc^{+}$ for 1 h in the $N_2$-saturated 0.1 M $TBAPF_6$ /DMF solution with acetic acid (30 mM) as the proton source (Fig. 7a). Then, the $H_2$ gas product was analyzed by GC. It was found that the reaction employing complex **1** as the electrocatalyst could generate significantly higher amount of $H_2$ than that using free $Ni^{2+}$ ions (Table 2). This result clearly showed that complex **1** was active toward the HER. Moreover, the stable current of -2.11 mA observed throughout the 1-h electrolysis indicated satisfactory stability of complex **1** under this operational condition (Fig. 7b). It should be noted that increasing the applied potential from -2.1 V to -2.3 V did not vastly improve %FE of catalyst **1**. Although the HER performance of complex **1** (40% FE) was in the lower end when compared to those of previously reported $Ni^{2+}$ complexes (46–94%FE)[37–40], the opportunity for other applications and several approaches for further development are still open such as ligand modification as well as molecular-catalyst immobilization onto carbonaceous materials.

Each reaction contains 1 mM catalyst in a $N_2$-saturated 0.1 M $TBAPF_6$ solution in DMF containing 30 mM acetic acid for 1 h electrolysis. %FE is the percentage of the Faradaic efficiency of the catalyst.

## Conclusions

We report the synthesis and characterization of novel pentadentate nickel(II) complexes featuring an acridine-based Schiff base ligand. The complexes were prepared *via* a nickel-promoted one-pot condensation of diphenylamine-2,2′-dicarboxaldehyde and TREN, accompanied by a ligand rearrangement at the head-unit motif. Consistent with the previous report by Brooker and co-workers, the rearrangement was proposed to proceed after Schiff-base condensation and facilitated by the nickel ions as a Lewis acid. The presence of the acridine moiety in the complexes was confirmed by X-ray crystallography with two distinct counterions and corroborated by the characteristic absorption band of acridine in UV-vis spectroscopy. Furthermore, the electrocatalytic hydrogen evolution reaction (HER) activity of a representative nickel(II) complex (**1**) was investigated. The complex demonstrated moderate HER activity in 0.1 M $TBAPF_6$ solution in DMF with the faradaic efficiency of 40% at -2.1 V vs. $Fc/Fc^{+}$ in the presence of acetic acid as the proton source.

This facile synthetic approach through the metal-mediated rearrangement of diphenylamine derivative presents a promising avenue for the rational design and facile synthesis of novel acridine-based ligands. Moreover, this strategy facilitates the exploration of these ligands and their corresponding metal complexes in various applications, including organic transformations, electro- and photocatalysis, and biological applications.

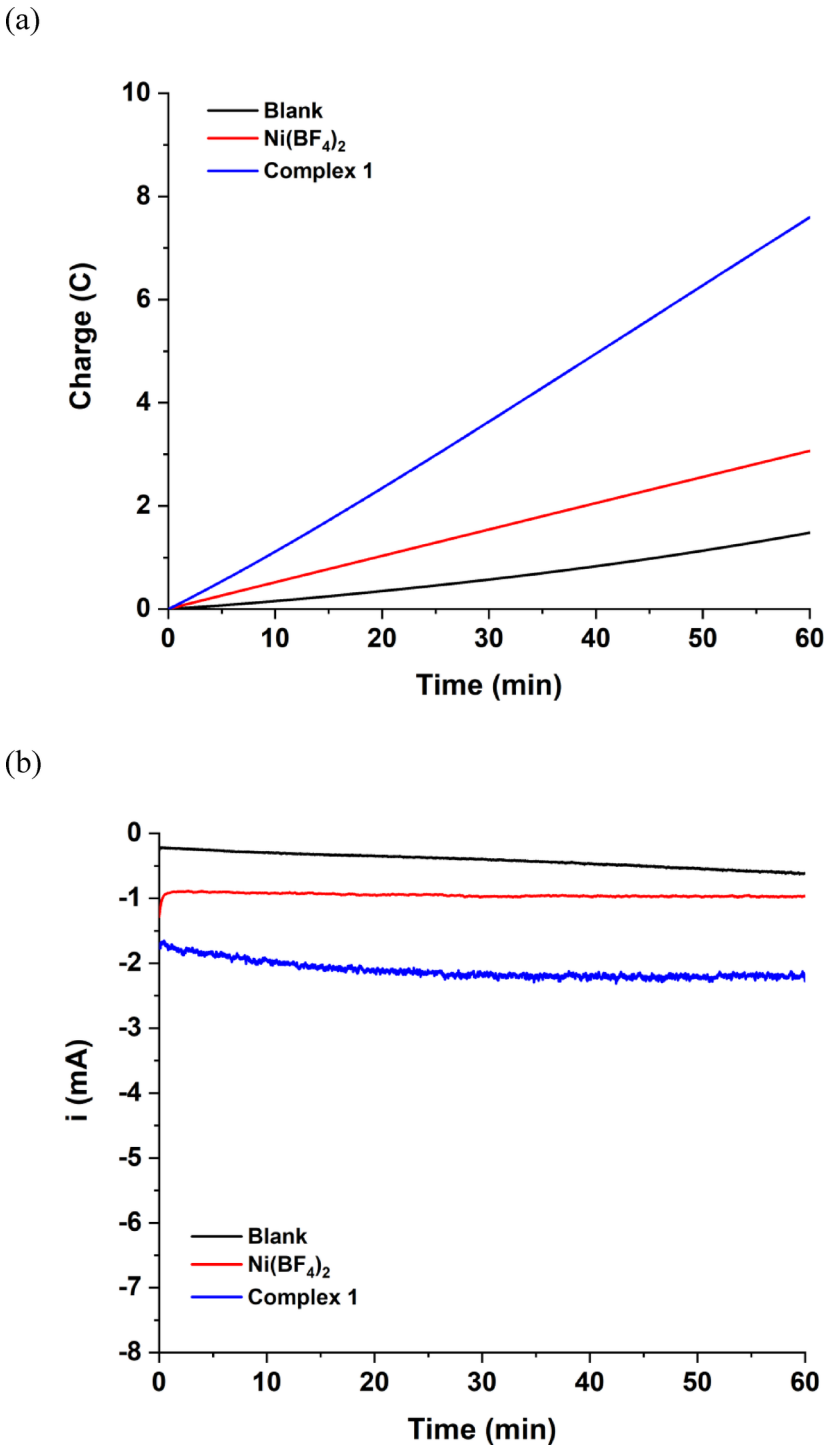


**Fig. 7**. Comparison of (**a**) charge accumulation profile and (**b**) current profile of the 1-h CPE in the absence of catalyst (blank, black line), and in the presence of $Ni(BF_4)_2$ (red line) and complex **1** (blue line) at -2.1 V vs. $Fc/Fc^+$ in a $N_2$-saturated 0.1 M $TBAPF_6$ solution in DMF containing 30 mM acetic acid.

| Catalyst | Charge / C | $H_2$ (μmol) | FE (%) |
|---|---|---|---|
| Blank | 1.5 | 2.5 | 32 |
| $Ni(BF_4)_2$ | 3.1 | 4.5 | 30 |
| **1** | 7.6 | 16.0 | 40 |

**Table 2**. Summarized catalytic activity of catalysts for HER at -2.1 V vs. $Fc/Fc^+$.

## Data availability

Data is provided within the manuscript or supplementary information files.

Received: 11 December 2024; Accepted: 28 April 2025
Published online: 06 May 2025

## References

1. Janockova, J. et al. Inhibition of DNA topoisomerases I and II and growth Inhibition of HL-60 cells by novel acridine-based compounds. *Eur. J. Pharm. Sci.* **76**, 192–202 (2015).
2. Oppegard, L. M. et al. Novel acridine-based compounds that exhibit an anti-pancreatic cancer activity are catalytic inhibitors of human topoisomerase II. *Eur. J. Pharmacol.* **602**, 223–229 (2009).
3. Aragoni, M. C. et al. $Zn^{2+}/Cd^{2+}$ optical discrimination by fluorescent acridine-based bis-macrocylic receptors. *Supramol Chem.* **29**, 912–921 (2017).
4. dos Santos Carlos, F., da Silva, L. A., Zanlorenzi, C. & Souza Nunes, F. A novel macrocycle acridine-based fluorescent chemosensor for selective detection of $Cd^{2+}$ in Brazilian sugarcane spirit and tobacco cigarette smoke extract. *Inorg. Chim. Acta* **508** (2020).
5. Marti-Centelles, V. et al. Fluorescent acridine-based receptors for $H_2PO_4^-$. *J. Org. Chem.* **77**, 490–500 (2012).
6. Dai, Y. et al. Acridine-based complex as amino acid anion fluorescent sensor in aqueous solution. *Spectrochim. Acta A.* **157**, 1–5 (2016).
7. Gunanathan, C. & Milstein, D. Selective synthesis of primary amines directly from alcohols and ammonia. *Angew Chem. Int. Ed. Engl.* **47**, 8661–8664 (2008).
8. Gunanathan, C., Shimon, L. J. W. & Milstein, D. Direct conversion of alcohols to acetals and $H_2$ catalyzed by an Acridine-Based ruthenium pincer complex. *J. Am. Chem. Soc.* **131**, 3146–3147 (2009).
9. Ye, X. et al. Alcohol amination with ammonia catalyzed by an acridine-based ruthenium pincer complex: a mechanistic study. *J. Am. Chem. Soc.* **136**, 5923–5929 (2014).
10. Daw, P., Ben-David, Y. & Milstein, D. Acceptorless dehydrogenative coupling using ammonia: direct synthesis of N-Heteroaromatics from diols catalyzed by ruthenium. *J. Am. Chem. Soc.* **140**, 11931–11934 (2018).
11. Das, S. & Thakur, A. J. A green development of Bernthsen 9-substituted acridine synthesis in the absence of solvent catalyzed byp-toluenesulphonic acid (p-TSA). *Green Chem. Lett. Rev.* **4**, 131–135 (2011).
12. Klemm, L. H., Chiang, E. & O'Bannon, G. W. Synthesis of an s-butyldibenz[a,h]acridine. Alkyl migration in the Bernthsen reaction. *J. Heterocycl. Chem.* **29**, 571–574 (1992).
13. Popp, F. D. Polyphosphoric acid in the Bernthsen Reaction1. *J. Org. Chem.* **27**, 2658–2659 (1962).
14. Su, Q. et al. Facile synthesis of acridine derivatives by ZnCl2-promoted intramolecular cyclization of o-arylaminophenyl schiff bases. *Org. Lett.* **16**, 18–21 (2014).
15. Malthus, S. J., Wilson, R. K., Larsen, D. S. & Brooker, S. Acridine-based ligands from cobalt(II) mediated rearrangement of diphenylamine-based starting materials. *Supramol Chem.* **28**, 98–107 (2015).
16. Juthathan, M. et al. Molecularly dispersed nickel complexes on N-doped graphene for electrochemical $CO_2$ reduction. *Dalton Trans.* **52**, 11407–11418 (2023).
17. Lafayette, E. A. et al. Synthesis, DNA Binding and Topoisomerase I inhibition activity of thiazacridine and imidazacridine derivatives. **18**, 15035–15050 (2013).
18. Brooker, S. *APEX3, SAINT and SADABS* (Bruker AXS Inc., 2016).
19. Spek, A. L. PLATON SQUEEZE: a tool for the calculation of the disordered solvent contribution to the calculated structure factors. *Acta Crystallogr. C Struct. Chem.* **71**, 9–18 (2015).
20. Sheldrick, G. M. SHELXT - integrated space-group and crystal-structure determination. *Acta Crystallogr. Found. Adv.* **71**, 3–8 (2015).
21. Sheldrick, G. M. Crystal structure refinement with SHELXL. *Acta Crystallogr. C Struct. Chem.* **71**, 3–8 (2015).
22. Dolomanov, O. V., Bourhis, L. J., Gildea, R. J., Howard, J. A. K. & Puschmann, H. OLEX2: a complete structure solution, refinement and analysis program. *J. Appl. Crystallogr.* **42**, 339–341 (2009).
23. Sanyal, R., Cameron, S. A. & Brooker, S. Synthesis and complexes of an N4 Schiff-base macrocycle derived from 2,2′-iminobisbenzaldehyde. *Dalton Trans.* **40**, 12277–12287 (2011).
24. Wilson, R. K. & Brooker, S. Complexes of a porphyrin-like $N_4$-donor Schiff-base macrocycle. *Dalton Trans.* **42**, 7913–7923 (2013).
25. Sickerman, N. S. et al. Synthesis, structure, and physical properties for a series of trigonal bipyramidal M(II)-Cl complexes with intramolecular hydrogen bonds. *Dalton Trans.* **41**, 4358–4364 (2012).
26. Sadhu, M. H., Solanki, A. & Kumar, S. B. Mixed ligand complexes of copper(II), cobalt(II), nickel(II) and zinc(II) with thiocyanate and pyrazole based tetradentate ligand: syntheses, characterizations and structures. *Polyhedron* **100**, 206–214 (2015).
27. Lau, N., Sano, Y., Ziller, J. W. & Borovik, A. S. Terminal Ni(II)-OH/-OH2 complexes in trigonal bipyramidal geometries derived from H2O. *Polyhedron* **125**, 179–185 (2017).
28. Malthus, S. J. et al. Carbazole-based N4-donor schiff base macrocycles: obtained metal free and as Cu(ii) and Ni(ii) complexes. *Dalton Trans.* **46**, 3141–3149 (2017).
29. Abudayyeh, A. M., Schott, O., Feltham, H. L. C., Hanan, G. S. & Brooker, S. Copper catalysts for photo- and electro-catalytic hydrogen production. *Inorg. Chem. Front.* **8**, 1015–1029 (2021).
30. Ilhan, S., Temel, H., Kilic, A. & Tas, E. Synthesis and spectral characterization of macrocyclic NiII complexes derived from various diamines, NiII perchlorate and 1,4-bis(2-carboxyaldehydephenoxy)butane. *Transition Met. Chem.* **32**, 1012–1017 (2007).
31. Kilic, A., Tas, E., Gumgum, B. & Yilmaz, I. Three new vic-dioxime ligands: Synthesis, characterization, spectroscopy, and redox properties of their mononuclear nickel(II) complexes. *Heteroat. Chem.* **18**, 657–663 (2007).
32. Yilmaz, I., Kilic, A. & Yalcinkaya, H. Synthesis, characterization, fluorescence and redox features of new vic-dioxime ligand bearing pyrene and its metal complexes. *Chem. Pap.* **62**, 398–403 (2008).

33. Kilic, A., Tas, E. & Yilmaz, I. Synthesis, spectroscopic and redox properties of the mononuclear $Ni^{II}$, $Ni^{II}(BPh_2)_2$ containing (B-C) bond and trinuclear $Cu^{II}$-$Ni^{II}$-$Cu^{II}$ type-metal complexes of *N,N′*-(4-amino-1-benzyl piperidine)-glyoxime. *J. Chem. Sci.* **121**, 43–56 (2009).
34. Jude Jenita, M., Thulasidhasan, J. & Rajendiran, N. Encapsulation of alkylparabens with natural and modified α- and β-cyclodextrins. *J. Incl. Phenom. Macrocyclic Chem.* **79**, 365–381 (2014).
35. Barma, A., Chakraborty, M., Bhattacharya, S. K., Ghosh, P. & Roy, P. Mononuclear nickel(II) complexes as electrocatalysts in hydrogen evolution reactions: effects of alkyl side chain lengths. *Mater. Adv.* **3**, 7655–7666 (2022).
36. Xu, H., Shang, H., Wang, C. & Du, Y. Surface and interface engineering of noble-metal-free electrocatalysts for efficient overall water splitting. *Coord. Chem. Rev.* **418**, 213374 (2020).
37. Fang, M., Engelhard, M. H., Zhu, Z., Helm, M. L. & Roberts, J. A. S. Electrodeposition from acidic solutions of nickel Bis(benzenedithiolate) produces a Hydrogen-Evolving Ni–S film on glassy carbon. *ACS Catal.* **4**, 90–98 (2014).
38. Chen, L. et al. Dual homogeneous and heterogeneous pathways in Photo- and electrocatalytic hydrogen evolution with Nickel(II) catalysts bearing tetradentate macrocyclic ligands. *ACS Catal.* **5**, 356–364 (2015).
39. Bergamini, G. & Natali, M. Homogeneous vs. heterogeneous catalysis for hydrogen evolution by a nickel(II) bis(diphosphine) complex. *Dalton Trans.* **48**, 14653–14661 (2019).
40. Niu, Z. et al. *Novel Dithiolene Nickel Complex Catalysts for Electrochemical Hydrogen Evolution Reaction for Hydrogen Production in Nonaqueous and Aqueous Solutions* 13230–241 (Electrocatalysis, 2022).


## Acknowledgements

This work was financially supported by the Research Cess Fund from Malaysia-Thailand Joint Authority (MTJA). N. P. gratefully thanked the Second Century Fund (C2F), Chulalongkorn University. We would also like to thank Professor Takashi Hayashi from the Department of Applied Chemistry, Graduate School of Engineering, Osaka University, Japan for helpful discussion. The authors acknowledge the Program Management Unit for Human Resources & Industrial Development, Research & Innovation (B41G670026).

## Author contributions

P.L. and M.J. conceived the study and designed the experiments. N.P. and M.J. performed the experiments, analyzed the data, and prepared the figures. K.C. and C.T. performed and analyzed the X-ray crystallographic data and prepared the related figures. P.T. and T.T. supervised and contributed to the discussion of the proposed mechanism and electrochemical studies. P.L., N.P. and M.J. wrote the initial draft of the manuscript. All authors contributed to the interpretation of the results and revised the manuscript.

## Declarations

## Competing interests

The authors declare no competing interests.

## Additional information

**Supplementary Information** The online version contains supplementary material available at https://doi.org/10.1038/s41598-025-00345-3.

**Correspondence** and requests for materials should be addressed to P.L.